Water Density Determination in High-Accuracy Flowmeter Calibration - Measurement Uncertainties and Practical Aspects

Rainer Engel
PTB Physikalisch-Technische Bundesanstalt, Department of Liquid Flow, Braunschweig, Germany
Tel:+49-531-592 1321, Fax:+49-531-592 69 1321, E-mail: rainer.engel@ptb.de

Hans-Joachim Baade
Dröge Baade Drescher Consulting Engineers, Salzgitter, Germany
Tel: +49-5341-2940-0 (direct access: -40), Fax: +49-5341-2940-44, E-mail: Baade@dbd-sz.de

Abstract: In liquid flowmeter calibration, the fluid density is one of the major quantities which impact the uncertainties in the measurement process of calibration. Thus, the in-process density determination in liquid flow standards reveals to be an essential component in the measurement uncertainty analysis.
In the case when a volume-reading flowmeter is calibrated against a gravimetric reference system, the accurate density value of the actual fluid applied in the calibration facility must be available, by measurement or computation, in order to convert the respective volumetric meter reading into an equivalent mass value. That is necessary as the reading of the meter under test (MUT) has to be compared with the reading of the gravimetric reference.
Additionally, fluid-density related impacts on the measurement uncertainty in a flow standard facility occur in the intermediate pipework which connects the meter under test with the reference device, i.e. the volumetric or gravimetric standard. Due to the difference in the thermal expansion coefficients of the pipework's material and the enclosed water, a systematic measurement deviation is caused if the temperature of the water and the pipework is varying during a calibration run. Practically, such temperature fluctuations always occur, due to varying ambient conditions and a more or less imperfect regulation of the water temperature in the flow facility. Thermal expansion implies a change in the fluid density. Thus, this effect, too, has to be taken into account for analyzing the measurement uncertainty of a flow standard facility.
This second density-related disturbing effect generally occurs in any calibration facility, regardless whether the meter reading is volume-related or mass-related, and in any combination with a gravimetric or volumetric reference standard.
A main issue of this paper is the practical aspect how to determine the water density in the calibration facility under real conditions or referred to real conditions and to derive approximation functions which describe the temperature behavior of water density and which are suitable to be applied for uncertainty analysis purposes.

Keywords: Liquid flow calibration, uncertainty analysis, water density uncertainty

1. Introduction – Uncertainty analysis

In liquid flow calibration, gravimetric-reference-based facilities represent high-accuracy flow standards. Regardless whether the flying- or standing-start-and-finish operating mode is combined with the static weighing method, the liquid density reveals to have a tremendous impact on measurement accuracy. Additionally, the material properties of several functionally relevant components, like the connecting pipework and the meter body contribute impacts on the system measurement uncertainty caused by thermal and mechanical stresses.

All these aspects of fluid density related impacts on the measurement uncertainty of a gravimetric liquid flow calibration facility represent the scope of this paper.

Generally, in fluid flow measurement applications, there may occur one of the following four types of **measurands**:

- (Average) Volume/**volumetric flow rate**: $$\overline{q}_V = \dot{V} = \frac{V_{REF}}{T_{MEAS}} = \frac{m_{REF}}{\rho_{Water} \cdot T_{MEAS}} \quad (1.1)$$
- (Average) **Mass flow rate**: $$\overline{q}_m = \dot{m} = \frac{m_{REF}}{T_{MEAS}} \quad (1.2)$$
- Total(ized) **volume measurement**: $$V_M = \int_0^{T_{MEAS}} \dot{V}(t)dt = \overline{q}_V \cdot T_{MEAS} \quad (1.3)$$
- Total(ized) **mass measurement**: $$m_M = \int_0^{T_{MEAS}} \dot{m}(t)\,dt = \overline{q}_m \cdot T_{MEAS} \quad (1.4)$$

Depending on the flow sensing principle applied and the meter make, the flowmeters that are subject of calibration in a flow facility may provide volume flow related (**Eqs. (1.1)** and **(1.2)**) or mass flow related (**Eqs. (1.3)** and **(1.4)**) measurement readings. The respective type of meter reading, volumetric or mass flow related, defines whether the value of liquid density is necessary to make the meter reading comparable to the mass reference reading.

However, in the flowmeter calibration process, not one of the above flow measurands, but the so-called meter **K-factor**, is subject of calibration:

$$K_{Meter} = \frac{f_{Output}}{\dot{V}_{REF}} \quad (1.5a)$$

$$K_{Meter} = \frac{N_{Pulses} / T_{MEAS}}{V_{REF} / T_{MEAS}} \quad (1.5b)$$

$$K_{Meter} = \frac{N_{Pulses}}{V_{REF}} \quad (1.5c)$$

The meter K-factor K_{Meter}, determined by applying **Eq. (1.5c),** is an average quantity, as its determination relies on pulse counting during the measurement time T_{MEAS}. While the pulse count N_{Pulses} is a representative value of the flowmeter reading f_{Output}, the reference volume V_{REF} is determined by diverter-operated flying-start-and-finish measurement with static weighing:

$$V_{REF} = \frac{m_1 - m_0}{\rho_{Water}} - \Delta V_{IP}(\vartheta, p) - \Delta V(\Delta T_{Error}) \quad (1.6)$$

The diverter operation delivers or defines the measurement time T_{MEAS} and, due to its operation principle **[1]**, the diverter is responsible for an erroneous volume deviation $\Delta V(\Delta T_{Error})$ which can be dedicated to an imperfect timer actuation, represented by the diverter timing error ΔT_{Error}.

Effects of fluctuating temperature and pressure within the pipework which interconnects the meter under test (MUT) and the gravimetric reference cause an additional contribution

$\Delta V_{IP}(\vartheta, p)$ to the deviations from an "exact" reference volume V_{REF} and, thus, are sources of measurement uncertainty.

The resulting equation discribing the reference flow rate in the calibration and measurement process is now as follows:

$$\dot{V}_{REF} = \frac{V_{REF}}{T_{MEAS}} = \frac{\frac{m_1 - m_0}{\rho_{Water}} - \Delta V_{IP}(\vartheta, p) - \Delta V(\Delta T_{Error})}{T_{MEAS}} \tag{1.7}$$

Inserting **Eq. (1.7)** into **Eq. (1.5a)** delivers the model equation that represents the complete measurement process for the meter K-factor determination. Further steps in the measurement analysis are the determination of the **standard uncertainty** and the **relative standard uncertainty**.

Then the standard uncertainty for meter K-factor K_{Meter} determination is as follows:

$$u^2_{K\_meter} = \left(\frac{\partial K_{Meter}}{\partial f_{Outout}} u_f\right)^2 + \left(\frac{\partial K_{Meter}}{\partial \dot{V}} \cdot \frac{\partial \dot{V}}{\partial m}\, u_m\right)^2 + \left(\frac{\partial K_{Meter}}{\partial \dot{V}} \cdot \frac{\partial \dot{V}}{\partial \rho_{Water}}\, u_\rho\right)^2 + \ \ldots$$
$$+ \left(\frac{\partial K_{Meter}}{\partial \dot{V}} \cdot \frac{\partial \dot{V}}{\partial (\Delta V_{IP})}\, u_{\Delta V}\right)^2 + \left(\frac{\partial K_{Meter}}{\partial \dot{V}} \cdot \frac{\partial \dot{V}}{\partial (\Delta V_{T\_Error})}\, u_{T\_Error}\right)^2 + \left(\frac{\partial K_{Meter}}{\partial \dot{V}} \cdot \frac{\partial \dot{V}}{\partial T_{MEAS}}\, u_T\right)^2 \tag{1.8}$$

When referring **Eq. (1.8)** to the meter K-factor K_{Meter}, the **relative standard uncertainty** of the measurement process is obtained is as follows:

$$\left(\frac{u_{K\_Meter}}{K_{Meter}}\right)^2 = \left(\frac{u_f}{f_{Output}}\right)^2 + \left(\frac{u_m}{m}\right)^2 + \left(\frac{u_\rho}{\rho_{Water}}\right)^2 + \left(\frac{u_{\Delta V}}{V_0}\right)^2 + \left(\frac{u_{T\_Error}}{V_0}\right)^2 + \left(\frac{u_T}{T_{MEAS}}\right)^2 \tag{1.9}$$

This type of an uncertainty model equation can be considered to represent the state of the art, i.e. it is generally applied for measurement uncertainty analysis in liquid flow standard facilities. However, it must be emphasized that, due to modular approach based on several sub-models, one measurand (e.g. the liquid temperature) may reveal to be the input quantity to more than one sub-model. In this case, it would mean that correlation effects will be implied so that a realistic evaluation the measurement, especially at low uncertainty levels, is not possible. At least, we must state that those uncertainty analysis results are not reliable.

In order to avoid those problems of "hidden" correlation effects, the size of sub-models must not be as small that any single measurand occurs as an input quantity to more than one sub-model. This approach is applied in this paper for analyzing the physical processes that occur within the pipework interconnecting the MUT and the gravimetric reference. **Eq. (5.2)** describes all the temperature and pressure related effects comprehensively.

2. Gravimetric liquid calibration facilities

The principal set-up of a gravimetric liquid flow calibration facility is shown in **Fig. 1**. As illustrated there, uncertainty impacts on the total measurement uncertainty of the calibration facility may be dedicated to the following factors of influence or subdevices **[1]**: flow generating system (electronically controlled pumps for providing adjustable and stable flow-rate operation),

meter under test (MUT), interconnecting pipe, flow diverter, water mass collection in the weighing tank, and the balance as the gravimetric reference.

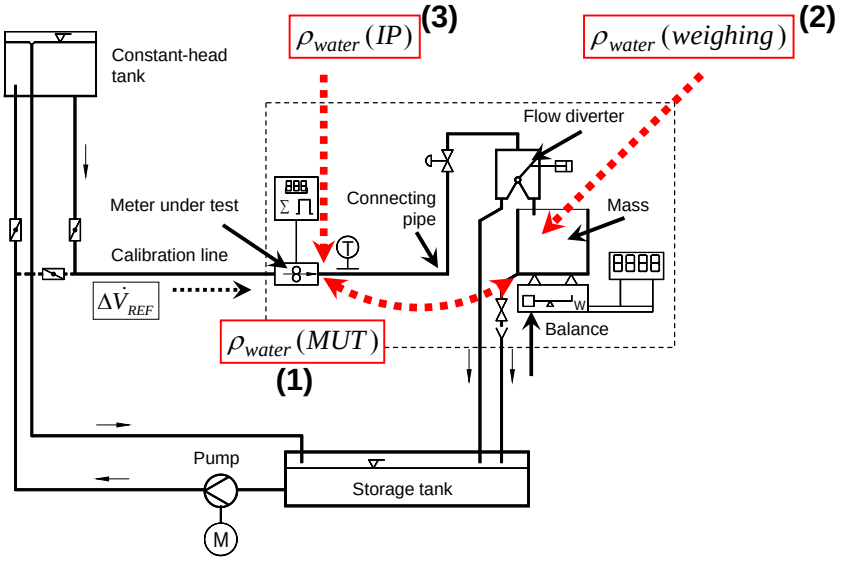

Figure 1 *Gravimetric liquid flow calibration facility – Uncertainty impacting items and impact of water density*
(1) *Converting m_{REF} into V_{REF}*
(2) *Weigh scale air buoyancy*
(3) *Material and fluid effects within the interconnecting pipework*

The motivation for the research work and experimental investigations, respectively, whose results are presented in this paper, was to improve the measurement capabilities of the high-accuracy water flow calibration facility at PTB Braunschweig (Germany's national metrological institute), i.e. the objective is to secure flow measurement and flowmeter calibration on an uncertainty level as low as possible.

Dedicated investigations and research work were performed in order to reduce the systematic and random effects caused by the diverting device and its operation, respectively. The situation prior to those improvements of the diverter operation is reflected by **Fig. 2a**. A model-based analysis and re-adjustment of the diverter parameters had been applied **[3]** and an essential improvement of the diverter operation was achieved.

A graphical representation of the measurement uncertainty analysis results that reflect the present situation, now, after certain diverter adjustments, is depicted in **Fig. 2b [3]**. Now it reveals that, as the present situation, the system's total expanded measurement uncertainty is dominated by the uncertainty contributions that result from water density related impacts.

In **Fig. 1**, there is indicated by the items **(1)** through **(3)**, which physical processes or effects do impact the measurement uncertainty of flowmeter calibration with a gravimetric flow standard facility:

1) Conversion of a volumetric flowmeter reading into an equivalent value of mass, in order to make the MUT reading comparable to the reference mass represented by the weigh scale reading, the gravimetric standard.

For that purpose it is necessary to provide a water density function that delivers accurate density values according to the fluid temperature which occur during a single calibration run within the MUT's meter body or in its very close downstream proximity. This issue is treated in **Subchapter 4.2** and **Appendix A.1**, respectively.

2) The systematic effects that are caused by fluctuations of the fluid temperature and pressure within the interconnecting pipework during a single calibration run.

Though being of deterministic nature, due to the uncertainties in determining the IP's exact volume, the uncertainties dedicated to temperature and pressure measurements, an absolutely exact calculation or correction of the volume of the fluid entering the IP and that which is leaving the IP during a calibration run, is not possible. Thus, these processes within the IP are additional sources which have an impact on the total uncertainty of the calibration process. This issue is described in **Chapter 5**.

3) The third "entry point", where water density causes an impact on the whole system's measurement uncertainty, is the gravimetric reference, the weigh scale.

Due to buoyancy effects, the weigh scale's reading is systematically influenced by the water and the ambient air densities during the measurement process and by the calibration weight's density and the ambient air density during the calibration of the weigh scale. These issues are subject of analysis and investigations in **Chapter 6**.

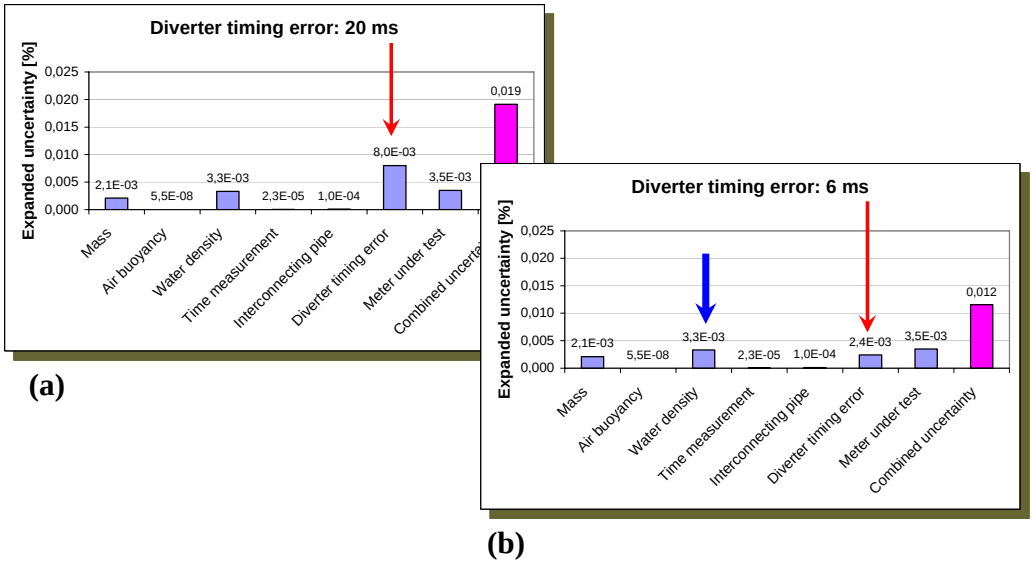

Figure 2 *Individual uncertainty contributions of the main quantities of impact to the total uncertainty of the calibration facility (PTB's water flow facility)* ***[3]***

a) *Effective diverter timing error prior to applying the model-based analysis*
b) *Diverter timing error after having applied corrections based upon model-based analysis approaches*

3. Modeling the density function of water as a test fluid in flow calibration facilities

3.1 Data and TANAKA model of the density of air-free water

ISO 4185 **[8]** provides data of the density of water in dependence of temperature, which are recommended to apply for the calculation of the measurement results and -uncertainty in water flow calibration facilities. Another source for water density data is ISO / TR 3663 **[9]**. Both data represent the density of Standard Mean Ocean Water (SMOW). Unfortunately neither ISO 4185 nor ISO / TR 3663 specify any expressions for the numeric approximation of the displayed data.

***Table 1**. Differences in temperature fix points between IPTS68 and ITS90*

ϑ_{90}	**°C**	0	10	20	30	40
$\vartheta_{90} - \vartheta_{68}$	**°C**	0.000	-0,002	-0,005	-0,007	-0,010

Furthermore ISO 4185 gives no declaration on the temperature scale, which is used with the published data; with respect to the issue of this standard, the application of ITPS-68 may be assumed.

Meanwhile a new temperature scale, the ITS-90, is established **[10, 11]** and is to be applied in metrology, and there are slight differences between the actual scale ITS-90 and the former scale IPTS-68. In the interesting temperature range between 0 °C up to 40 °C, the differences do not exceed -0.010 K, see **Table 1**.

Due to scientific correctness, for highly accurate measurements this difference should be taken into account, even if the impact on the density is really insignificant as the following example depicts: the difference of density between 20.000 °C and 20.005 °C is only -0.001033 kg/m³ and that is considerably smaller then the below mentioned uncertainty of the density measurement of PTB's test rig.

A widely recommended equation for the computation of the density of liquid water is given by TANAKA **[4]**. Water density is to be computed in terms of the ITS-90 as follows:

$$\rho_{TANAKA}(\vartheta) = A_5 \cdot \left[1 - \frac{(\vartheta + A_1)^2 \cdot (\vartheta + A_2)}{A_3 \cdot (\vartheta + A_4)} \right] \tag{3.1}$$

$A_1 = -3.983035°C$

$A_2 = 301.797°C$

$A_3 = 522528.9°C$

$A_4 = 69.34881°C$

$A_5 = 999.974950 kg/m^3$

ϑ in $°C$

Eq. (3.1) fits the actual reliable data of the density of water within a limit of expanded uncertainty (k=2) of max. $0.88 \cdot 10^{-3}$ kg/m³ **[4]**, representing data of SMOW. SMOW is a special quality of water collected in the oceans and then it is purified and de-aerated in a subsequent special procedure. If water of other qualities than SMOW is used, TANAKA suggests fitting the factor A_5 for an optimum representation of the data of the currently used water.

3.2. Plant-related aspects – dissolved atmospheric gas and water compressibility

Water is able to dissolve gases, in this particular case ambient air. According to Henry's law, the more the pressure will rise, the more air will be dissolved. But even if test facilities are sometimes run under higher pressures, air will be dissolved only at a level of ambient atmospheric pressure, because the storage tank is (mostly) run under ambient pressure with connection to the ambient atmosphere and no source of air under a higher pressure level for dissolving any air is present. Thus, for further calculations the effect caused by dissolved air under ambient pressure is taken into account.

TANAKA **[4]** furthermore published expressions for correction-terms for the allowance of impacts on the density due to the saturation of the water by dissolved air and due to the compressibility of the water.

The summand for considering dissolved air is given by:

$$\Delta\rho_{diss\_air}(\vartheta) = s_0 + s_1 \cdot \vartheta \tag{3.2}$$

$$s_0 = -4.612 \cdot 10^{-3}\ kg/m^3$$

$$s_1 = 0.106 \cdot 10^{-3}\ kg/(m^3 °C)$$

and the factor for the consideration of compressibility, respectively:

$$\Delta\rho_{Compr} = f(p,\vartheta) = 1 + \left(k_0 + k_1 \cdot \vartheta + k_2 \cdot \vartheta^2\right) \cdot \left(p - p_0\right) \tag{3.3}$$

$$p_0 = 101325\ Pa$$

$$k_0 = 50.74 \cdot 10^{-11}\ /Pa$$

$$k_1 = -0.326 \cdot 10^{-11}\ /(Pa \cdot °C)$$

$$k_2 = 0.004161 \cdot 10^{-11}\ /(Pa \cdot °C^2)$$

Combining these expressions, the density is to be calculated in full by **Eq. (3.4)**:

$$\rho_{TANAKA}(\vartheta, p) = \left\{ A_5 \cdot \left[1 - \frac{(\vartheta + A_1)^2 \cdot (\vartheta + A_2)}{A_3 \cdot (\vartheta + A_4)} \right] + (s_0 + s_1 \cdot \vartheta) \right\} \cdot \left(1 + \left(k_0 + k_1 \cdot \vartheta + k_2 \cdot \vartheta^2\right) \cdot (p - p_0)\right) \tag{3.4}$$

In accordance to the recommendations by CIPM and EURAMET **[12, 13]** for the subsequent considerations below the equation of TANAKA **[4]** is used as well as the baseline for the comparisons as for further calculations.

For consideration of the effect of compressibility, a typical operation pressure of approx. 3 bars is assumed. Both effects on the density of the water are computed by application of the above mentioned equations and the results are shown in **Fig. 3**. The impact of dissolved air is quit tiny; but the influences of compressibility and quality of the water should cause a major impact and are to be taken into account. Special attention is required to the impact of the quality and origin of the water. This will be gathered below.

Fig. 3 shows a summarized arrangement of the above stated facts in form of a deviation plot as follows:

The relative differences $(\rho^* - \rho_{TANAKA}) \cdot 10^6 / \rho_{TANAKA}$ are plotted vs. temperature (ITS-90), where ρ^* is a placeholder for the different items under comparison as depicted in **Fig. 3**.

It can be seen, that the data of ISO 4185 and ISO / TR 3663 agree well and are represented by the equation of TANAKA et al. within a tolerance band of approx. $5 \cdot 10^{-6}$. Dissolved air lowers the density slightly, whilst the increase of density by rising pressure should not be neglected.

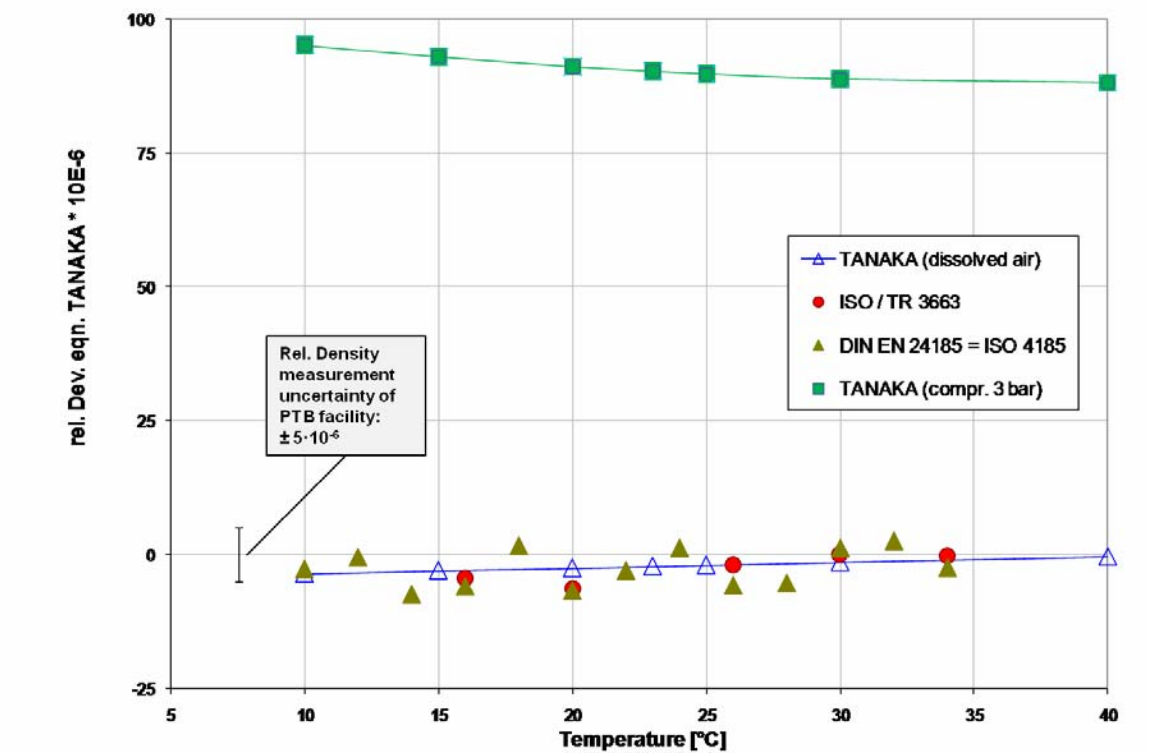

Figure 3 *Effect of dissolved air and compressibility on density of water (comparison / deviation)*

4. Survey of different water sample densities and different ways of approximation

4.1 An "exact" approximation

Water of the above described SMOW quality is not available for use in flowmeter calibration facilities. Thus, water of local origin is used, mostly delivered by the public utility suppliers or pumped from own sources, fore instance from own wells.

These waters are of different quality, they disagree in their chemical and physical properties, in this particular case of interest the density is varying within a noticeable range. **Fig. 4** depicts the relative deviations in density between samples of waters in comparison to the density, given by the equation of TANAKA, respectively. These water samples had been collected from several locations throughout Germany. The density measurements were performed with a DMA 500 type densitometer (manufacturer: Anton Paar Company, Austria), which is used with the Hydrodynamic Test Field at PTB. The relative uncertainty of the density measurements is approx. $5 \cdot 10^{-6}$ $(k = 2)$. The results of these comparative measurements are presented in **Fig. 4**.

The densities of the different analysed water samples are considerably greater than the density of SMOW. The determined relative increase of the density covers a range up to $8 \cdot 10^{-4}$ and exceeds the uncertainty of the density measurement at the test rig in the order of a factor of approx. 150! This impact cannot be neglected, if high-precision measurements are aimed at. A noticeable

systematic error is caused if high-precision measurements are carried out without precise density determination.

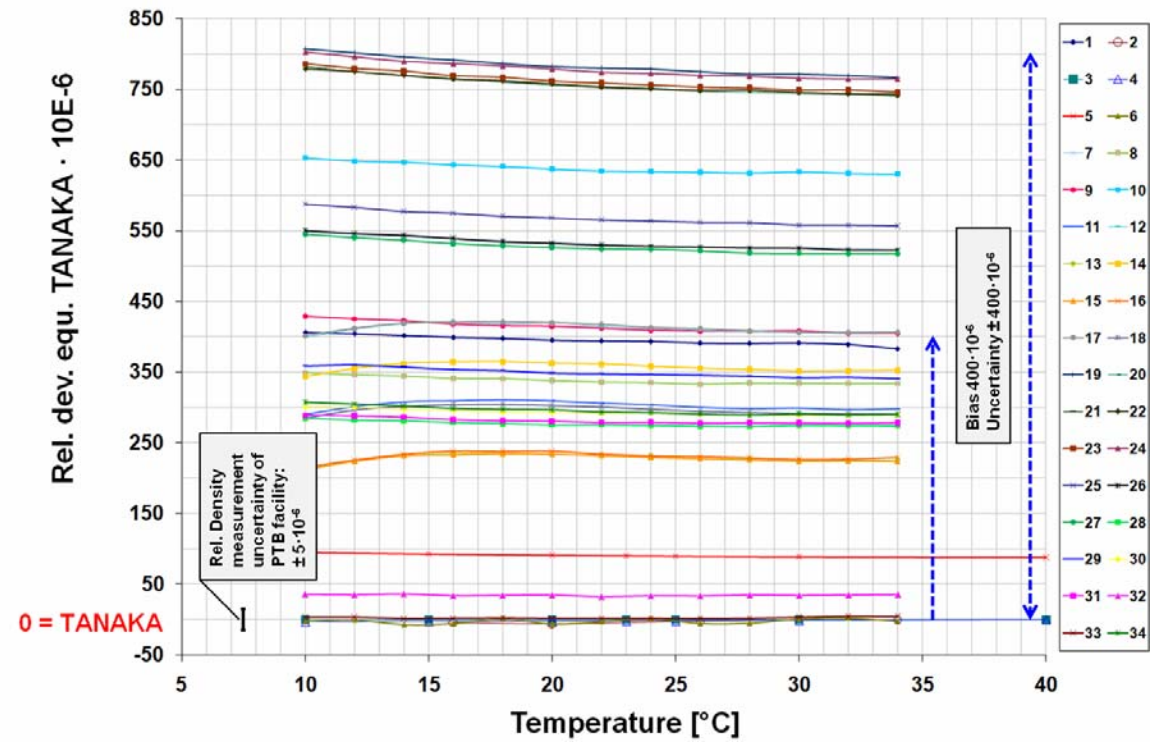

Figure 4 *Densities of water samples from several different laboratories and local water suppliers (Detailed information referring to the sources, see **Appendix A.3.**)*

For further considerations of the measurement uncertainties of flowmeter calibration facilities, the reader will be confronted with a survey of a best-case and a worst-case scenario, depending on whether the density is determined precise by measurements of the actual used test water of the rig or if the density is taken into account only by using a "standard formula" without any relation to the used water. This impact reveals an increase of the uncertainty of the density from $\pm 20 \cdot 10^{-6}$ % (including numerical approximation errors) as a best case scenario up to $(400 \pm 400) \cdot 10^{-6}$ % as a worst case scenario, if the density of the water is unknown and a mean value is to be used. In this case a bias of $400 \cdot 10^{-6}$ % is to be taken into account, which is superposed by an uncertainty of $\pm 400 \cdot 10^{-6}$ % as shown in **Fig. 4**. In this case the overall uncertainty is computed by an approach given in **[15]** as follows:

$$u = k \cdot \sqrt{s^2 + \delta^2 / 3} \qquad (4.1)$$

The bias is represented by δ and the uncertainty by s. The expansion factor k is suggested to be set to 2 **[15]**. In this case the absolute uncertainty becomes 0.92 kg/m³, the relative uncertainty $924 \cdot 10^{-6}$, respectively.

4.2. Practical density approximation function of water actually used in the test facility

The approach of in-process water density determination which is utilized in PTB's high-accuracy water flow facility (hydrodynamic Test Field) relies on water density approximation functions

that are determined prior to the flowmeter calibration measurements on the basis of real process density data **[16]**. For that purpose, a water sample is automatically taken from the process or test fluid, respectively, circulating in the calibration plant by a laboratory densitometer, initiated by the supervising process control system or, individually, on the operator's command.

This densitometer (type DMA 5000, manufacturer: Anton Paar Company, Austria) is programmed that it delivers pairs of data, comprising temperature and dedicated density values $\vartheta_{Cal,i}$ and $\rho_{Cal,i}$ on the *i*-th test point. Within the temperature range 10 °C through 34 °C, thus, there are available 13 pairs of data which are now the basis for a least-square fit applied to an 3rd degree polynomial approximation function **[5]**:

$$\rho_{Approx}(\vartheta_{Water}) = f(\vartheta_{Cal,i}, \rho_{Cal,i}, \vartheta_{Water}) \tag{4.2a}$$

$$\rho_{Approx}(\vartheta_{Water}) = a_0 + a_1 \cdot \vartheta_{Water} + a_2 \cdot \vartheta_{Water}^2 + a_3 \cdot \vartheta_{Water}^3 \tag{4.2b}$$

$$\begin{aligned} \rho_{Approx}(\vartheta_{Water}) &= a_0(\vartheta_{Cal,i}, \rho_{Cal,i}) + a_1(\vartheta_{Cal,i}, \rho_{Cal,i}) \cdot \vartheta_{Water} + \ldots \\ &\ldots + a_2(\vartheta_{Cal,i}, \rho_{Cal,i}) \cdot \vartheta_{Water}^2 + a_3(\vartheta_{Cal,i}, \rho_{Cal,i}) \cdot \vartheta_{Water}^3 \end{aligned} \tag{4.2c}$$

As shown in **Appendix A.1**, it has proven that:

- a 3rd-order polynomial approximation function is sufficient for the an approximation within the temperature range from 10 °C to 34 °C; in comparison to the ISO standard-based approximation function (5th order, air-free water **[17]**) it represents a reduced temperature range;
- a higher order of the polynomial approximation function does not improve generally the quality of the computed density values.

According to the ISO Guide to the expression of uncertainty in Measurement **[2]**, **Eq. (4.2)** represents the model of the water density determination based on an approximation function, with the random input variables $\vartheta_{Cal,i}$, $\rho_{Cal,i}$ and ϑ_{Water}. These quantities are obtained from the densitometer or acquired by means of the temperature sensor which is installed in the pipework of the calibration facility.

The combined uncertainty is obtained by forming the partial from **Eq. (4.2c)** and inserting them into **Eq. (4.3)**:

$$\left[u(\rho_{Approx})\right]^2 = \left[\frac{\partial \rho_{Approx}}{\partial \vartheta_{Cal,i}} \cdot u(\vartheta_{Cal,i})\right]^2 + \left[\frac{\partial \rho_{Approx}}{\partial \rho_{Cal,i}} \cdot u(\rho_{Cal,i})\right]^2 + \left[\frac{\partial \rho_{Approx}}{\partial \vartheta_{\mathrm{Pr}ocess}} \cdot u(\vartheta_{\mathrm{Pr}ocess})\right]^2 \tag{4.3}$$

As the derivation of the sensitivity coefficients (differential quotients) on an analytical way reveals to be extremely sophisticated and cumbersome, these coefficients were determined by applying the difference quotients approach, utilizing the capabilities of EXCEL spread sheets.

For a 3rd-order polynomial approximation function whose coefficients were calculated on the basis of the temperature-density data pairs, which were acquired from the densitometer, following parameters had been determined **[5]**:

- **Sensitivity coefficient** with respect to the $\vartheta_{Cal,i}$ values: **$-6.6435 \cdot 10^{-6}$ kg/m³K**
- **Sensitivity coefficient** with respect to the $\rho_{Cal,i}$ values: **1.9995 kg/m³/(kg/m³)**
- **Sensitivity coefficient** with respect to the ϑ_{Water} values: **$-2.0817 \cdot 10^{-1}$ kg/m³K**

- **Numerical approximation error** (relative): **± 2.0·10^{-6}**

As there are no further information than the maximum deviations (errors), the probability distributions functions of the above estimates are assumed to be rectangular.

The estimates of the above random input variables are obtained from the specification data sheet of the densitometer:

Uncertainty related device parameters of the type DMA densitometer

- **Temperature reading**: $\vartheta_{Cal,i}$ **= ± 10 mK** (rectangular probability distribution)
- **Density reading:** $\rho_{Cal,i}$ **= ± 0.05 kg/m³** (rectangular probability distribution)

The third random input variable, the temperature of the water passing through the MUT, is acquired via a temperature sensor which is installed in the pipework of the water flow facility.

The measurement uncertainty which is dedicated to the water temperature determination originates both from the temperature measurement chain and from fluid flow related impacts due to time fluctuations of flow and spatial temperature distribution in the pipe's cross section.

In the simulation computations whose results are presented in **Chapter 7**, uncertainty values of ± 0.3 °C and ± 0.6 °C are applied as alternative parameters.

5. Water density as an impact to the interconnecting pipe effect

5.1. Physical model and derived relations

In order to model the impacts of the water density's temperature and pressure behavior, it is assumed that the interconnecting pipe (IP) volume (IP) V_{IP} between the meter under test (MUT) and the reference standard consists of a straight pipe section, as shown in **Fig. 5a**. The size of this IP volume is defined both by the distance which has to be bridged between MUT and reference and by the pipe diameter which is necessary for a defined maximum flow rate to pass through. Thus, the IP's volume, generally, reveals to be a parameter of the facility that cannot be chosen freely. The lack of knowledge with respect to the "exact" size of IP's volume δV_{IP} represents a factor of uncertainty which must be taken into account in a measurement analysis which refers to uncertainty effects in the IP section.

This idealized pipe section may consist of subsections which were made of different materials each, with different thermal expansion coefficients.

The magnitude of the IP's volume will vary in the case of varying temperature according to the thermal expansion coefficient of the material which the pipe section consists of.

In addition, pressure changes within the pipe section will affect the pipe's diameter. The effects due to both thermal effects and pressure effects are summarized in $\pm \Delta V_{IP}$ (**Fig. 5b**).

The effects described here are of systematic nature and corrections can be applied. However, due to the uncertainties that have to be dedicated to the quantities which act as input variables, these effects represent sources of uncertainty which may impact the total measurement uncertainty of the whole calibration facility tremendously. Effects of the several parameters which are of interest for practical applications were investigated and the results of the numerical simulations are depicted in the **Figures 7** through **10**.

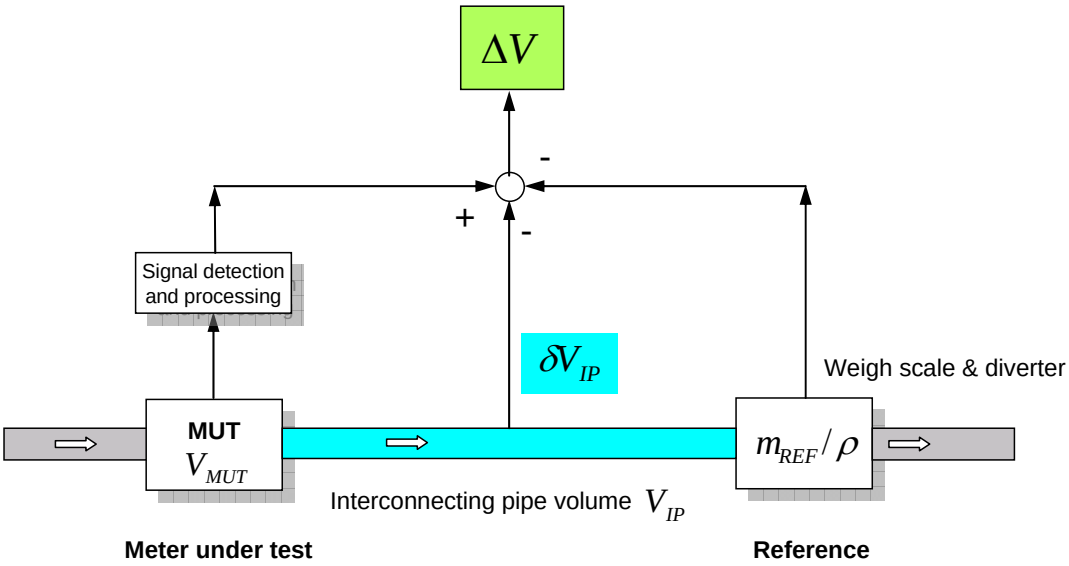

a)

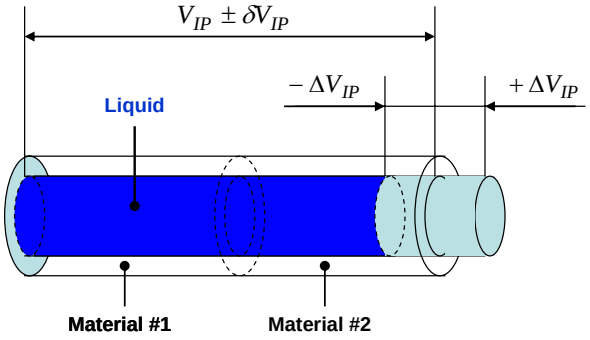

b)

Figure 5 *Measurement impacts of the interconnecting pipework*

a) *The interconnecting pipe volume as an element in the measurement process*
b) *Simplified model of the interconnecting pipework*

5.2. Temperature and pressure impacts

5.2.1. Temperature and pressure impacts on the inclosing pipework

The interconnecting pipe volume and the content of the enclosed volume of water will change by temperature and pressure effects. Rising temperature will increase the volume due to thermal expansion of the pipe material, if the coefficient of thermal expansion of the pipe's material is positive.

Pressure rise within the pipe section will increase the pipe diameter due to its elastic properties. This is to be considered..

Both effects are explained in detail and calculated exactly in **Appendix A 2**.

5.2.2. Temperature and pressure impacts on the enclosed water and entrapped air

In addition to the above mentioned effects, the enclosed water will change its density depending on temperature and pressure as depicted in **Chapter 3**.

If the pipe system is not carefully exhausted, finally a further effect has to be considered to that all: the possibly entrapped air is subject to the same changes of temperature and pressure as the water and the pipe material and thus the gas bubbles will change their volume. Even for this case, further physical details are explained in **Appendix A 2**, respectively.

5.2.3. Interaction of pipe and fluid effects

With regard to the claimed level of uncertainty, the above mentioned effects must to be taken under consideration, and this was done in detail, see **Appendix A 2**. As the result the change of the interconnecting pipe volume is expressed as follows:

$$\Delta V_{IP} = V(\vartheta_{finish}, p_{finish}) - V(\vartheta_{start}, p_{start}) \tag{5.1}$$

$$\Delta V_{IP} = \frac{\pi}{4} \cdot \left[d_i + \frac{\left(p_{finish} - p_0\right) \cdot d_i^{\,2}}{2 \cdot w \cdot E} \right]^2 \cdot l \cdot \left[1 + 3 \cdot \alpha \cdot \left(\vartheta_{finish} - \vartheta_0\right)\right] - \ldots\ldots$$
$$\ldots\ldots - V_{air,0} \cdot \frac{p_0}{p_{finish}} \cdot \frac{\vartheta_{finish} + 273.15}{\vartheta_0 + 273.15} - V_{start} \tag{5.2}$$

The overall measurement uncertainty of the calibration facility is impacted among others by the change and uncertainty of the volume of the interconnecting pipe, which is now to be considered as a sub-model of the entire facility. By this way, the exact determination of the contribution of the interconnecting pipe subsystem to the total uncertainty budget of the entire facility now is possible using the regular procedures of uncertainty calculations:

For the estimation of the combined uncertainty of the volume of water within the interconnecting pipe, the impacts of each given quantity are to be taken into account. The probability distributions for all quantities are of rectangular type, thus the divisor is 1.73.

Thus in this special case, quantities affected by considerable uncertainties are:

- the determination of the pipe volume VIP
- the determination of the entrapped air volume V_{air}
- the process variables as the temperatures t and t_0
- the process variables as the pressures p and p_0
- the linear thermal coefficient of expansion of the pipe material α
- the elastic modulus of the pipe material E
- the thickness of the wall of pipe w,

- in total at least 9 quantities.

5.2.4. Practical aspects – Subdivision of the interconnecting pipework

This paragraph has been added with the intension to show that the model of uncertainty effects which is presented in this paper relies on a simplified structure of the plant installations within the interconnecting pipe section. In reality, there is, at least, one flow-regulating valve which is installed in this part of the pipework.

In the case, if lower measurement uncertainties are subject and objective of the uncertainty analysis, i.e. uncertainties which are significantly lower than in the case of this paper, a “more realistic” approach to the real situation of the pipework installations has to be applied in order to take into account all physical effects which impact the measurement process. As shown in **Fig. 6**,

if one regulating valve is part of the IP, we will find subsections (defined by the subvolumes V_1 through V_3) which are affected by different temperatures (T_1 … T_3) and pressures (p_1 … p_3). In this case, the model of the IP volume effects will contain further sub-models in the hierarchy of the measurement uncertainty analysis procedure, which implies a more sophisticated uncertainty model. Part of the variables that have to be introduced in order to describe the processes, generally, are not accessible by measurement. Thus, this real approach of an uncertainty model, on principle, increases the accuracy of quantitative description of the system behaviour. However, the lack of information, due to process variables which are not measured or are nor measurable, reduces the benefits of the utilization of such a detailed, "realistic" model.

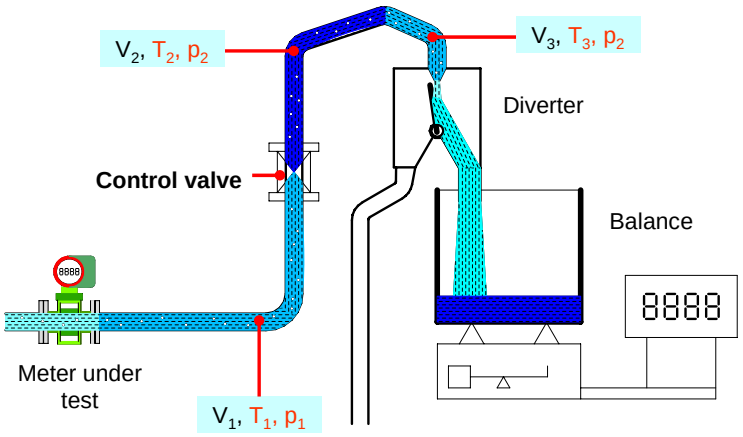

Figure 6 *Approaching to a more realistic model of the interconnecting pipework*
- *"existence" of subsections due to the presence of control valves*
- *changing process conditions: pressure and temperature*

6. Buoyancy effects in a gravimetric reference

6.1. Basic relations

If the mass of any body is determined by a weighing system located in a gravitational field and within a surrounding atmosphere, the weighing result is influenced by the buoyancy effect. That means the indication of the weighed mass is reduced by the weight of air, which is displaced by the body of the test piece to be weighed. The weight of the displaced air is given by the displacing air volume of the body to be weighed multiplied by the density of the displaced ambient air. For high precision measurements, this effect has to be considered, otherwise a systematic error occurs.

The volume of water within the respective weighing tank in charge is to be determined by **Eq. (6.1)**:

$$V_{REF} = \frac{1-\dfrac{\rho_{Amb\_air,Cal}}{\rho_{cal\_weight}}}{1-\dfrac{\rho_{Amb\_air,Meas}}{\rho_{water}}} \cdot \frac{m_{Cal\_weight}}{\rho_{water} \cdot W_{Cal\_weight}} \cdot [W_1 - W_0] \qquad (6.1)$$

where W_1, W_0 and W_{Cal_weight} are the readings of the weigh scale during the states of load, tare and calibration against the dead load mass m_{Cal_weight}, respectively. $\rho_{Amb\_air,Meas}$ and ρ_{water} are the

densities of ambient air and the weighed water during measurement process and they represent the buoyancy correction according to the weighing process whilst $\rho_{Amb\_air,Cal}$ and ρ_{cal_weight} are the above mentioned density of ambient air and of the calibration weights during calibration process, expressing the buoyancy correction for this process.

A simple and very rough correction of buoyancy can be applied by using the density of the air at ambient standard atmosphere conditions, i.e. at a temperature of 20 °C, a pressure of 1,013.25 mbar and a relative humidity of 50 % the density of the ambient air is 1.2 kg/m³. The uncertainty of this correction does not meet the challenging requirements for high precision measurements. Thus, two more precise solutions are discussed below.

6.2. "Exact" solution

The density of ambient air is computed by use of the simplified exponential version of CIPM-formula, for further details see: Guidelines on the Calibration of Non-Automatic Weighing Instruments **[7]**:

$$\rho_{Amb\_air} = \frac{0.34848 \cdot p_{amb} - 0.009 \cdot h_{amb} \cdot \exp(0.061 \cdot \vartheta_{amb})}{273.15 + \vartheta_{amb}} \quad \left[\mathrm{kg/m^3}\right] \tag{6.2}$$

With:

- ambient air temperature: ϑ_{amb} [°C]
- ambient barometric pressure: p_{amb} [mbar]
- ambient relative humidity: h_{amb} [%]

This formula yields results with $u_{formula}/\rho_{amb\_air} \leq 2.4 \cdot 10^{-4}$ under the following conditions of ambient variables (uncertainties of the measurements of p_{amb}, h_{amb}, and ϑ_{amb} are not included and have to be taken into account by measurement uncertainty analysis):

- 600 mbar $\leq p_{amb} \leq$ 1,100 mbar
- 20 % $\leq h_{amb} \leq$ 80 %
- 15 °C $\leq \vartheta_{amb} \leq$ 27 °C

As ambient conditions are really measured, the buoyancy correction is to be applied exactly with the determination of reference mass. This causes the most precise results.

6.3. Worst-case assumption

If ambient conditions are not determined by monitoring or process measurements, for buoyancy calculations a rough estimation of ambient conditions and related uncertainties for industrial laboratory environment are taken from Guidelines on the Calibration of Non-Automatic Weighing Instruments **[7]**:

- ambient air temperature: $\vartheta_{amb} = (22 \pm 5)$ °C
- ambient barometric pressure: $p_{amb} = 1013.12 - z \cdot 0.12 \pm 40$ [mbar]
  (at a height z [m] above sea level)
- ambient relative humidity: $h_{amb} = (50 \pm 30)$ %

In this case, the considerable higher contribution to measurement uncertainty is to be considered.

7. Case studies and analysis results

In order to analyze the water density, interconnecting pipe and buoyancy effects, as described above, following cases, which represent typical application aspects, were investigated by means of numerical simulations:

- **Case #1** - "**Ideal"** conditions: (**Fig. 7**)
  - **exact knowledge** of the IP's volume (V_{IP} = 500 l)
  - **no entrapped air** within the interconnecting pipework
  - uncertainty in **temperature measurement** ($\Delta\vartheta = \pm 0.3°C$)
  - "exact" **approx. of the water density** ($\Delta\rho/\rho = \pm 2 \cdot 10^{-5}$)
  - balance full scale reading (**3.000 kg**)

- **Case #2 -"Optimum"** conditions: (**Fig. 8**)
  - **uncertain knowledge** of the IP's volume ($\Delta V_{IP} = \pm$ 1 l)
  - **no entrapped air** within the interconnecting pipework
  - uncertainty in **temperature measurement** ($\Delta\vartheta = \pm 0.6°C$)
  - "exact" **approx. of the water density** ($\Delta\rho/\rho = \pm 2 \cdot 10^{-5}$)
  - reduced weigh scale range (**2.500 kg**)

- **Case #3** - **Real** conditions 1: (**Fig. 9**)
  - **uncertain knowledge** of the IP's volume ($\Delta V_{IP} = \pm$ 1 l)
  - **entrapped air** within the IP (V_{air} = 1 l)
  - uncertainty of the **entrapped air volume** ($\Delta V_{air} = \pm$ 1 l)
  - uncertainty in **temperature measurement** ($\Delta\vartheta = \pm 0.6°C$)
  - **water density approximation** based on tolerance band $\Delta\rho/\rho = (400 \pm 400)\ 10^{-5}$
  - reduced weigh scale range (**2.500 kg**)

- **Case #4** - **Real** conditions 2: (**Fig. 10**)
  - **uncertain knowledge** of the IP's volume ($\Delta V_{IP} = \pm$ 1 l)
  - **entrapped air** within the IP (V_{air} = 1 l)
  - uncertainty of the **entrapped air volume** ($\Delta V_{air} = \pm$ 1 l)
  - uncertainty in **temperature measurement** ($\Delta\vartheta = \pm 0.6°C$)
  - **water density approximation** based on tolerance band $\Delta\rho/\rho = (400 \pm 400) \cdot 10^{-5}$
  - reduced weigh scale range (**500 kg**)

Cases #1 through **#4** are to show what impacts on the total measurement uncertainty of a gravimetric flow facility are caused by:

- (Lack of) knowledge with respect to absolute magnitude of the IP's volume, represented by $\pm\Delta V_{IP}$;
- Entrapped air within the interconnecting pipework V_{air} and its uncertainty $\pm\Delta V_{air}$;

- Uncertainty of temperature measurement within the interconnecting pipe section $\pm \Delta \vartheta$ (comprises both time responses and spatial distribution);
- Uncertainty in the measurement (determination) of the fluid (water) density $\pm \Delta \rho / \rho$ which is representative or valid during a single calibration run (measurement process);
- Impacts of liquid compressibility and dissolved air in the fluid had been subject of investigation, too, but no explicit results in form a diagram are present in this paper. With respect to liquid compressibility effects, see final statement in **Chapter 8**.

As there are no specific information on the properties of the above random-like "input" quantities, generally, designated here as X_i, they are assumed to provide rectangular probability distribution functions. The respective probability parameters $\pm \Delta X_i$ were applied for the uncertainty analysis calculations.

The uncertainty in temperature measurement $\pm \Delta \vartheta$ originates both from the uncertainty which is provided by the temperature measurement chain devices and from temperature fluctuations due to an imperfect operation of the temperature regulating devices.

According to **Fig. 7**, which represents the simulation results of **Case #1**, we can recognize that, under ideal conditions - as summarized above - in our exemplified model, the total measurement uncertainty is significantly impacted by the uncertainty of the diverter operation, defined by its diversion timing error $\pm \Delta T_{div}$.

One essential prerequisite to realize **ideal measurement conditions**, i.e. low-uncertainty calibrations, is that the liquid density determination is based upon an "exact" approximation function, as described in **Chapter 4.1**.

When comparing the simulation results in **Fig. 8** with **Fig. 7**, it becomes obvious that a lack of knowledge (i.e. uncertainty) with respect to the magnitude of interconnecting pipe volume causes a significant increase in the total facility measurement uncertainty. Though other parameter being modified simultaneously in the simulation computations, the effect of $\pm \Delta V_{IP}$ is dominating combined uncertainty in **Case #2**.

Case #3 demonstrates that, as shown in **Fig. 9**, entrapped air in the interconnecting pipework and a rough approximation function of the water density lead to a further significant increase in total system measurement uncertainty. Especially, the rough density-temperature approximation function, which relies on the diagram in **Fig. 4**, reveals to be an impact factor that leads to a significant higher increase of the system uncertainty.

As visualized in **Fig. 10**, which depicts the situation of **Case #4**, the utilization of a reduced degree of weigh tank filling (example: one sixth of full scale reading) is a tremendous uncertainty increasing impact factor.

The above cases represent only a limited choice of the wide range of combinations of possible impact factors, their magnitudes, and their probability distribution factors.

The abbreviations standing for the sources of uncertainty in the previous **Figures 7** through **10** are explained in the legend table below.

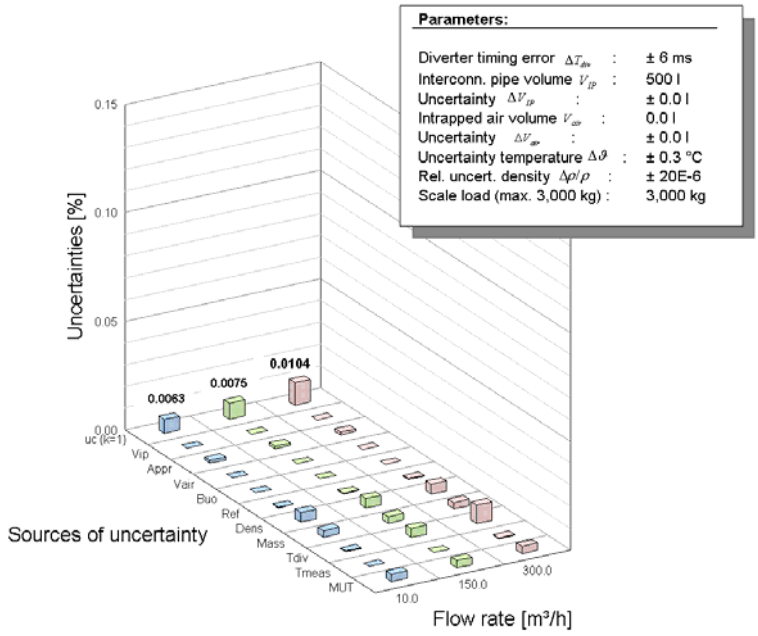

Figure 7 *Sources of uncertainty and their impact on the facility's total uncertainty*
*- **Ideal conditions**: exact knowledge of the IP's volume **and** no entrapped air within the interconnecting pipework*
*(For explanations and definitions of the abbreviations applied on the diagram's abscissa, see the table following the 4 diagrams: **Legend of abbreviations**)*

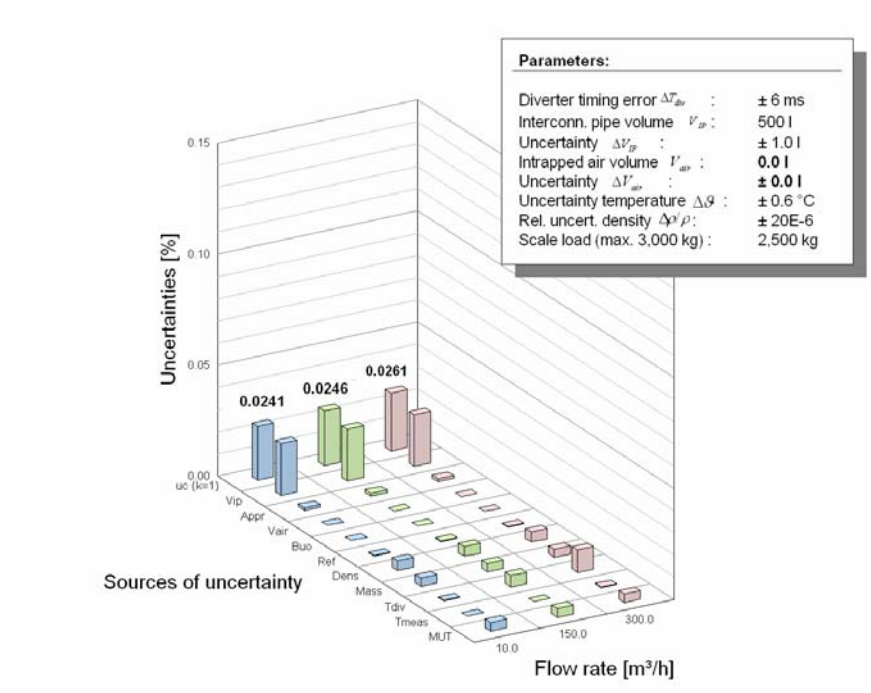

Figure 8 *Sources of uncertainty and their impact on the facility's total uncertainty*
*- "**Optimum" conditions**: no entrapped air within the interconnecting pipework*

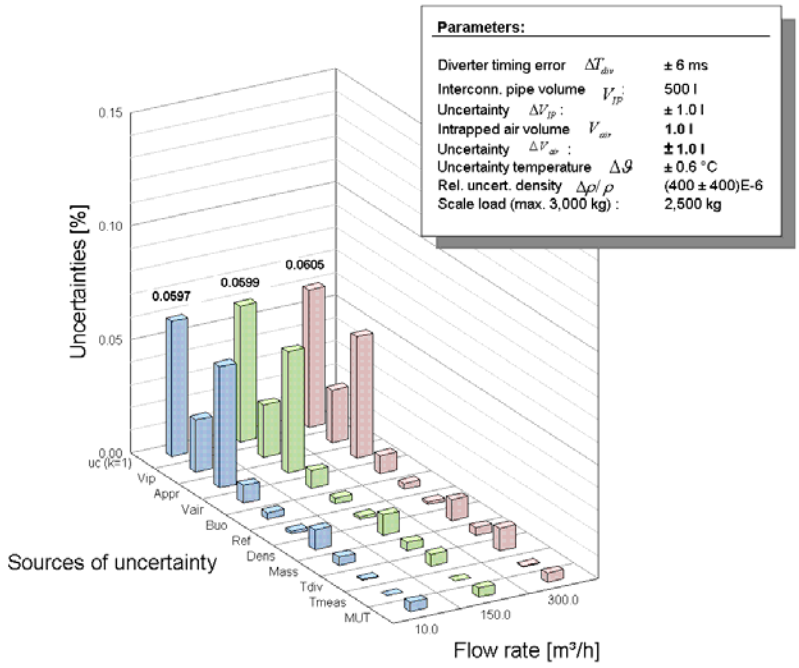

Figure 9 *Sources of uncertainty and their impact on the facility's total uncertainty - **Real conditions**: entrapped air within the interconnecting pipework*

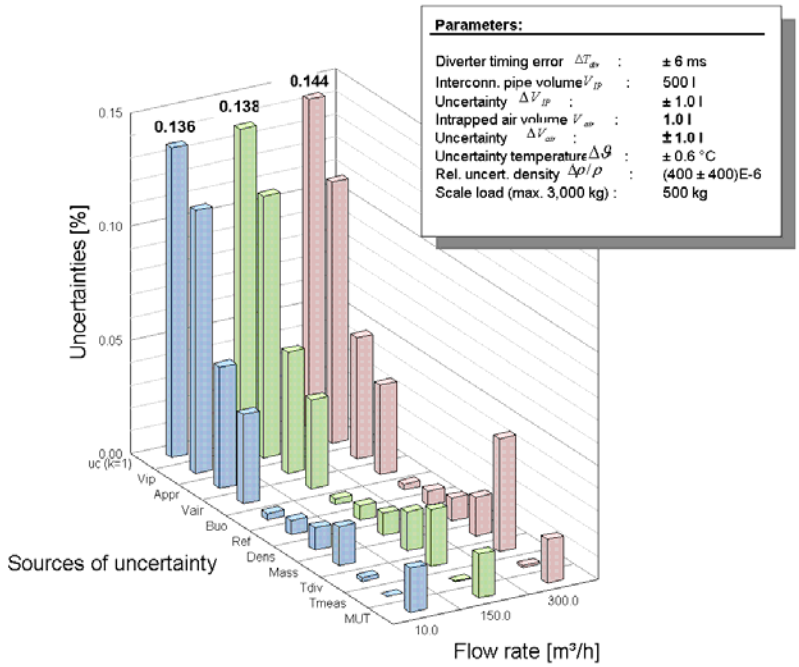

Figure 10 *Sources of uncertainty and their impact on the facility's total uncertainty - **Real conditions**: entrapped air and reduced weigh scale range*

Legend: Abbreviations (abscissa) applied in **Figures 7** through **10**

Abbreviation	Symbol / Meaning	Definition
uc(k=1)	u_c	Combined standard uncertainty (relative values, k = 1)
Vip	V_{IP}	Uncertainty of the determination of the IP's volume
Appr	Approximation	Type of approximation of the water density function and magnitude of the water density $\Delta\rho / \rho$
Vair	V_{air}	Parameter that indicates whether entrapped air occurs within the IP's volume, if YES than it represents the uncertainty of the volume of entrapped air
Buo	Buoyancy	Buoyancy impacted by the densities of water, calibration mass pieces, and ambient air
Ref	Reference	Summarizing all reference conditions as one component e.g. the reference mass pieces for weigh scale calibration or the uncertainty of the initial data for calculating the IP's volume
Dens	Density	Uncertainty of water density
Mass	Mass	Uncertainty contributed due to the uncertainty in determining the mass of collected water in the weigh tank
Tdiv	T_{Div}	Diverter's timing error
Tmeas	T_{MEAS}	Measurement time, diverter operated water collection of water in the weigh tank
MUT	Meter under test	Uncertainty contributions caused by the MUT, only comprises those effects due to the meter's signal resolution according to its meter K-factor and that part of measurement repeatability which can be dedicated to the MUT

Parameters and simulation input data: See tables "Parameters" inserted in **Figures 7** through **10**

8. Discussion and conclusions

- Exact values of the densities and their functional dependencies from temperature are generally only available for ideal fluids, i.e. in case of water flow facilities, exact functions are only existent for double distilled water and Standard Mean Ocean Water, respectively.
- For high-accuracy applications, the density's function vs. temperature must be determined on the basis of measurements with water samples taken from the facilities.
- Practical boundary conditions result from the individual designs of the calibration facilities and their operation conditions. Due to the operation principles of the control valves, which are arranged downstream of the MUT in the interconnecting pipe (IP) section between MUT and the reference standard, under certain process conditions, degassing might be caused. Degassing enhances air as bubbles or dissolved air in the test fluid. Both, air bubbles in the liquid and dissolved air, result in a decreased effective liquid density.
- As model analysis calculations revealed, dissolved air in the test fluid causes an insignificant impact on measurement uncertainty of a water flow facility. Thus, this effect can be neglected without an impact on practical uncertainty analysis results.

- The most significant impact of liquid density on the facility's accuracy is due to the fact that in calibrating a volume-reading flowmeter against a gravimetric standard, the meter reading must be transferred in a mass-related equivalent.
- Temperature dependent properties like the density of the test fluid and the IP material's thermal expansion coefficient cause a systematic deviation between the fluid quantity that passes through the MUT and that which reaches the reference standard during the measurement and water collection time.
- The compressibility of the test fluid, due to pressure effects in the pipework, cannot be neglected without causing a loss in accuracy or an underestimation of the facility's measurement uncertainty.
- Practically the interconnecting pipework is not an end-to-end pipe volume, but for the operation of a flow facility, control valves are located in this section. That implies a more sophisticated functional model for measurement uncertainty analysis purposes than the assumption of single pipe volume. This fact must be emphasized.
- Buoyancy in the weighing process is affected both by the liquid density and the ambient air density. But the above effects, where water density is involved as a factor of impact, do more significantly impact the magnitude of the total measurement uncertainty of a gravimetric flow facility than the buoyancy effects in the weigh process.
- When deriving the functional relations of the physical processes involved, in the case of a single process quantity (e.g., the liquid temperature) that impacts several sub-models as an input quantity, the basic model equation must be developed so comprehensively that the respective quantity finally represents a single input to the respective sub-model as the smallest subset that can be created.
- In the measurement uncertainty models describing liquid flow calibration, generally, correlation effects occur. This results from the fact that, in the case of sub-models being applied in a modular system analysis approach, a single measurand is often the input quantity to several sub-models. The comprehensive models presented in this paper, inherently, take into account those physical interrelation effects, so that they do not require a separate treatment and analysis as correlation effects.

Legend

Symbol	Definition	Unit
$a_j(\vartheta_{Cal,i}, \rho_{Cal,i})$	**Coefficients** of the density approximation function, j = 0 … 3	$(kg/m^3)/(°C)^j$
A_1	**Coefficient** of the TANAKA density formula	°C
A_2	dito	°C
A_3	dito	°C
A_4	dito	°C
A_5	dito	kg/m^3
c	**Sensitivity coefficient**	
d_i	**Inner diameter** of interconnecting pipe	m
E	**Elastic modulus** of pipe material	N/m^2
f_{Output}	**Frequency**, signal output of the MUT	Hz
h_{amb}	**Relative humidity** of ambient air	%
k	**Expansion factor**	---
k_0	**Correction coefficient for compressibility** of water, TANAKA density formula	1/Pa

k_1	dito	1/(Pa·°C)
k_2	dito	1/(Pa·°C²)
K_{Meter}	**Flowmeter K-factor**	Pulses/m³, pulses/kg
l	**Length** of interconnecting pipe	m
m_0	**Weigh scale tare load** prior to water collection	kg
m_1	**Mass of water** after fluid collection in the weigh tank	kg
m_{REF}	**Reference mass,** represented by the quantity water collected in the weigh tank during T_{MEAS}, $m_{REF} = m_1 - m_0$	kg
m_{Cal_weight}	**Mass of calibration weights**	kg
$\dot{m}$	**Mass flow rate**	kg/s
N_{Pulses}	**Pulse count**, acquired from the MUT meter output during T_{MEAS}	/
p	**Pressure**	Pa, bar, mbar
p_0	**Reference pressure** (101.325 Pa)	Pa, bar, mbar
p_{amb}	**Pressure of ambient air**	mbar
$\overline{q}_m$	(Average) **Mass flow rate**	kg/s
$\overline{q}_V$	(Average) **Volumetric flow rate**	m³/h
s	**Uncertainty** of density determination	kg/m³
s_0	**Correction coefficient for dissolved air** in water, TANAKA density formula	kg/m³
s_1	dito	kg/(m³·°C)
T	**Temperature**	K
T_{MEAS}	**Measurement**, diverter-operated actuation of the water collection in the weigh tank	s
u	**Uncertainty** of density determination	kg/m³
$u(\rho_{Approx})$	**Combined uncertainty** of the output of the approx. function	kg/m³
$u(\vartheta_{Cal,i})$	**Standard uncertainty** of temperatures from densitometer	°C
$u(\rho_{Cal,i})$	**Standard uncertainty** of densities from densitometer	kg/m³
$u(\vartheta_{Process})$	**Standard uncertainty** of in-process temperature determination	°C
V_{air}	**Volume of entrapped air**	l
ΔV_{air}	**Uncertainty of the entrapped air volume**	l
V_{IP}	**Volume of interconnecting pipe**	m³
δV_{IP}	**Uncertain information** (lack of knowledge) of the size of the IP volume	m³
ΔV_{IP}	**Uncertainty of the IP's volume**	m³
V_{REF}	**Reference volume**, as the equivalent to the reference mass	kg
$\dot{V}$	**Volumetric flow rate**	m³/h
$\Delta V(\Delta T_{Error})$	**Volume error**, due to diverter operation characteristics	mm
w	**Wall thickness** of interconnecting pipe	mm
W_1	**Reading of the weigh scale** during state of load	*Digits*/N
W_0	**Reading of the weigh scale** during state of tare	*Digits*/N
W_{Cal_weight}	**Reading of the weigh scale** during state of calibration	*Digits*/N
$\frac{\partial \rho_{Approx}}{\partial \vartheta_{Cal,i}}$	**Sensitivity coefficient** of the approx. function with respect to temperature values delivered from the densitometer	(m³/h)/°C
$\frac{\partial \rho_{Approx}}{\partial \rho_{Cal,i}}$	**Sensitivity coefficient** of the approx. function with respect to density values delivered from the densitometer	(m³/h)/ (m³/h)

$\frac{\partial \rho_{Approx}}{\partial \vartheta_{Process}}$	**Sensitivity coefficient** of the approx. function with respect to the temperature which is measured during flow calibration	(m³/h)/°C
Greek letters		
α	**Linear coefficient of thermal expansion** of pipe material	1/°C
ϑ	**Temperature**	°C
ϑ_0	**Reference temperature** (20 °C)	°C
ϑ_{68}	**Temperature according to IPTS 68**	°C
ϑ_{90}	**Temperature according to ITS 90**	°C
$\vartheta_{Cal,i}$	**Temperature** adjusted at the i-th test point where $\rho_{Cal,i}$ is determined by the densitometer	°C
ϑ_{amb}	**Temperature** of ambient air	°C
ϑ_{Water}	**Water temperature** within the calibration facility during measurement	°C
δ	**Bias** of density determination,	kg/m³
Δ	**Difference**	
$\rho_{Cal,i}$	**Density** determined by the densitometer and which is dedicated to the *i*-th test point and $\vartheta_{Cal,i}$, respectively	g/cm³
ρ_{cal_weight}	**Density of the calibration weights**	kg/m³
ρ_{water}	**Density of water**	kg/m³
ρ_{Amb_air}	**Density of ambient air**	kg/m³
$\rho_{Amb\_air,Cal}$	**Density of ambient air** during weigh scale calibration process	kg/m³
$\rho_{Amb\_air,Meas}$	**Density of ambient air** during the measurement process	kg/m³

Acknowledgement

The authors would like to thank Mr. A. Eggestein from PTB Braunschweig for having performed the measurements which delivered the data used for the analysis of the water density approximation functions, and, thus, provided a contribution to the realization of this paper.

References

[1] Engel, R., Baade, H.-J., Model-based flow diverter analysis for an improved uncertainty determination in liquid flow calibration facilities, *Measurement Science and Technology*, 21 (2010), (11pp), 2010. *[http://iopscience.iop.org/0957-0233/21/2/025401]*

[2] JCGM member organization (BIPM, IEC, IFCC, ILAC, ISO, IUPAC and OIML) 2008 Evaluation of measurement data - Guide to the expression of uncertainty in measurement JCGM 100:2008, *[http://www.bipm.org/utils/common/documents/jcgm/JCGM_104_2009_E.pdf]*

[3] Engel, R., Further improvements in the measurement uncertainty of PTB's Hydrodynamic Test Field, *PTB web site,]*, PTB Braunschweig, 2010. *[http://www.ptb.de/en/org/1/nachrichten1/2010/fundamentals/htf.htm]*

[4] Tanaka, M., Girard, G., Davis, R., Peuto, A. and Bignell N. Recommended table for the density of water between 0 °C and 40 °C based on resent experimental reports, *Metrologia*, 2001 , 38, 301-309.

[5] Engel, R., Measurement uncertainty of PTB's water flow calibration facility, *unpublished research report*, PTB Braunschweig, 2005.

[6] Coleman, H.W., Steele, W.G., Experimentation and Uncertainty Analysis for Engineers, 2nd Edition, John Wiley & Sons, Inc., New York, 1999.

[7] Guidelines on the Calibration of Non-Automatic Weighing Instruments EURAMET/cg-18/v.02 *[http://www.euramet.org/fileadmin/docs/Publications/calguides/EURAMET_cg-18_v.02.pdf]*

[8] ISO 4185, Measurement of liquid flow in closed conduits - Weighing method, International Organization for Standardization 1980

[9] ISO / TR 3663, Viscosity of Water, International Organization for Standardization 1998

[10] The International Temperature Scale of 1990 (ITS-90), Procès-verbaux du Comité International des Poids et Mesures, 78th meeting, 1989

[11] Preston-Thomas, H., The International Temperature Scale of 1990 (ITS-90, *Metrologia* 1990, 27, 3 - 10

[12] Harvey, A.H., Span, R., Fujii, K., Tanaka, M., Davus, R. S., Density of water: roles of the CIPM and IAPWS standards, *Metrologia*, 2009, 46, 196 - 198

[13] Guidelines on the determination of uncertainty in gravimetric volume calibration, *EURAMET calibration guide* / cg-19 / v.01, September 2009 *[http://www.euramet.org/fileadmin/docs/Publications/calguides/EURAMET-cg-19-01_Guidelines_in_uncertainty_volume.pdf]*

[14] Roark, Raymond J., Formulas for Stress and Strain, 4th Edition, McGraw-Hill Book Company, New York, 1965

[15] Kacker, R., Sommer, K.-D., Kessel, R., Evolution of modern approaches to express uncertainty in measurement, *Metrologia*, 2007, 44, 513 – 529

[16] Engel, R., Baade, H.-J., Rubel, A., Performance improvement of liquid flow calibrators by applying special measurement and control strategies, *Proceedings of the 11th International Conference on Flow Measurement FLOMEKO 2003*, Groningen, The Netherlands, May 12-14, 2003. *[http://www.ptb.de/de/org/1/15/152/papers/hdp_control_flome_03.pdf]*

[17] Bettin, H., Spieweck, F., Die Dichte des Wassers als Funktion der Temperatur nach Einführung der Internationalen Temperturskala von 1990, *PTB-Mitteilungen*, 100 3/90, 195-196

8. Appendices

Appendix A.1. Derivation of the practical density approximation function and uncertainty estimation

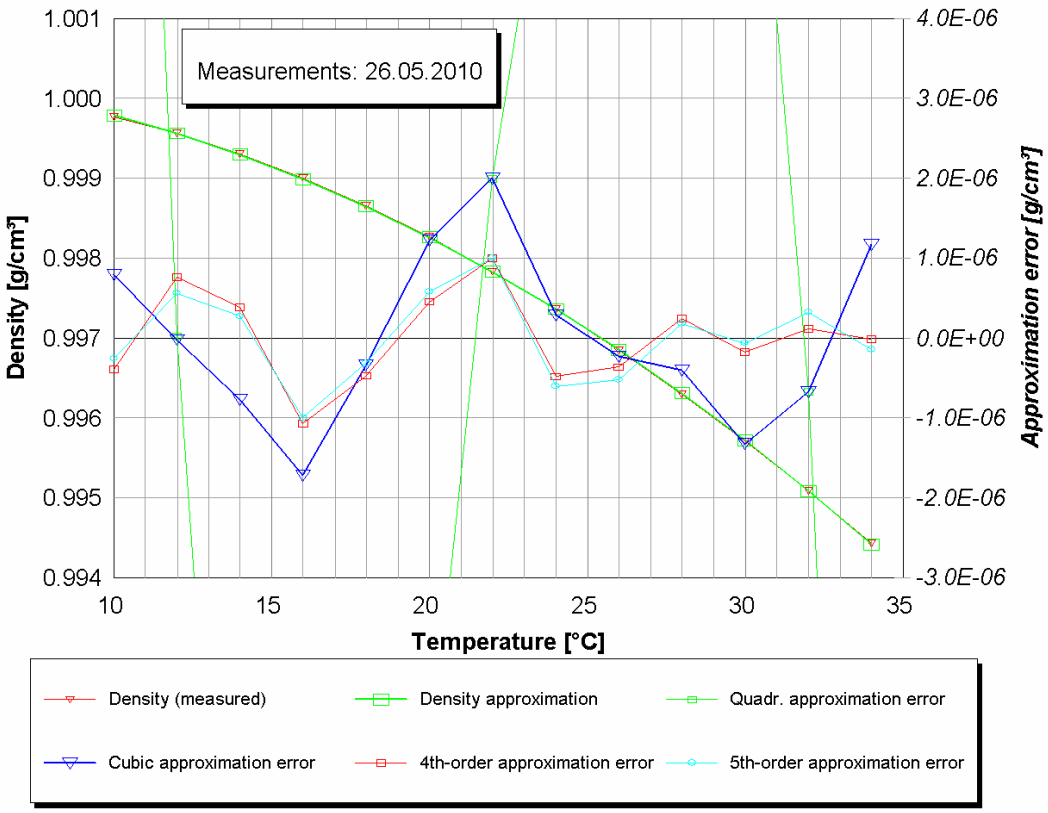

Figure A.1 *Practical water density approximation function: temperature range 10 °C through 34 °C*
(demonstration of the effect of different orders of the polynomial approximation function)

In this appendix chapter, it is shown that the polynomial approximation function, which was introduced in **Subchapter 4.2**, represents a mathematical model which provides an accuracy level that satisfies the requirements of measurement uncertainty analysis for water flow facilities. As **Fig. A.1** reveals, a 3rd-order polynomial approximation provides an acceptable accuracy level which is characterized by the numerical approximation errors whose magnitudes are lower than $|\pm 2{\cdot}10^{-6}|$. This numerical approximation error represents one component that contributes to the uncertainty caused by applying an approximation function (**Chap. 4.2**). Furthermore, it can be recognized in **Fig. A.1** that an increase of the order of the polynomial function does not reduce the maximum numerical approximation error significantly. That is the reason why a polynomial order of three had been considered to be suitable for modeling the water density as a function of temperature. According to the application condition with PTB's high-accuracy water flow facility [16], the water temperature is adjustable by setpoint-control within a range from 10 °C through 35 °C.

The error curves depicted in **Fig. A.2** prove that the 3rd-order polynomial approximation, generally, delivers water density approximation values whose maximum numerical errors are

below | ± 2·10^{-6}|. The approximation functions and the error curves, which are shown there, rely on water samples that were taken on several days, immediately prior to flow calibration measurements.

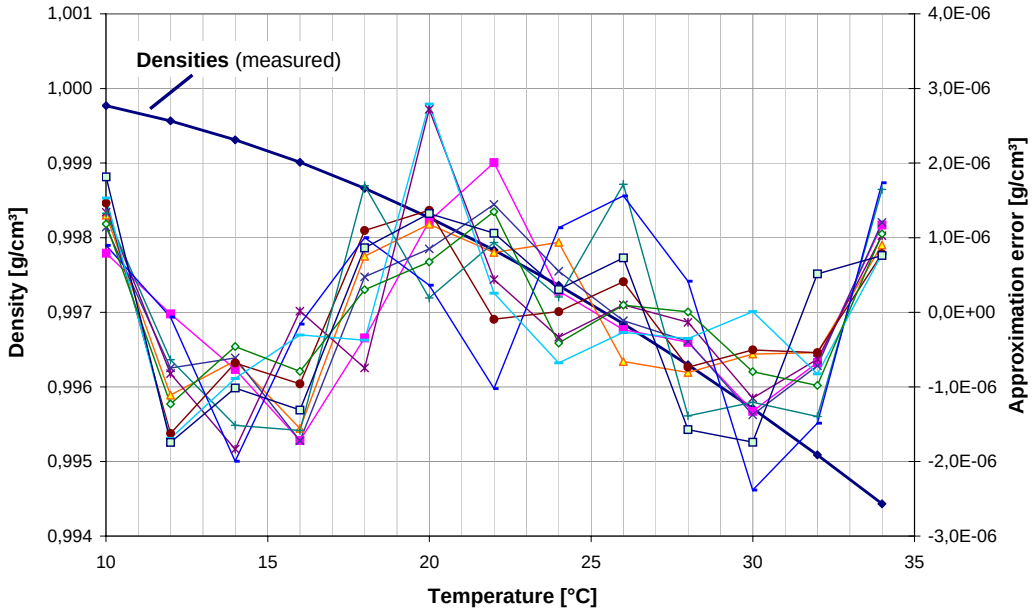

Figure A.2 *Practical water density function: 3rd-ordere polynomial approximation function*
- Water densities, measured
- Approximation errors

Appendix A.2. Derivation of the physical relations that characterize the process in the interconnecting pipework

The volume of the interconnecting pipe and the content of enclosed fluid respectively is consisting of different sections with different dimensions and (slightly) different operating conditions of temperature and pressure (See also: **Fig. 6**):
Section between MUT and control valve

1. Section between MUT and control valve
2. Section between control valve and top of the feeding pipe to the diverter
3. Section between top of the feeding pipe down to the diverter's nozzle outlet

For simplification it will be represented by only one common section, but under consideration of all influencing factors and relevant physical effects. They are

1. Geometric volume
2. Temperature effects (impacting the thermal expansion of the pipe material and volume, respectively (effect 2))
3. Pressure effects (impacting the pipe volume due to mechanical stress of the pipe's wall (effect 3))
4. Air bubbles (They are reducing the effective water volume (effect 4a). Additionally the gaseous volume of entrapped air is affected as well by its compressibility (effect 4b) as thermal expansion (effect 4c))

5. Surface tension (A check of this interaction between air bubbles and liquid fluid reveals this effect of negligible order: either the size of the bubbles is tall and in this case the effected internal pressure rise within the bubbles is very small and therefore negligible - or in the other case the bubbles are tiny and, although then the internal pressure rise within the bubbles is high, the entrapped volume of gas is very small and then this quantity is negligible.)

The model equation of the interconnecting pipe is derived as follows.

The nominal volume is given by:

$$V_{IP,0} = \frac{\pi}{4} \cdot d_i^{\,2} \cdot l \qquad \text{(A 2.1)}$$

with the inner diameter d_i and the length $\boldsymbol{l}$ at reference conditions ϑ_0 and $\boldsymbol{p_0}$.

Due to the internal pressure $\boldsymbol{p}$ (effect 3), the wall becomes radial displaced and the diameter increase is expressed by **[14]**:

$$\Delta d_i = \frac{\left(p - p_0\right) \cdot d_i^{\,2}}{2 \cdot w \cdot E} \qquad \text{(A 2.2)}$$

where $\boldsymbol{w}$ is the thickness of the pipe's wall and $\boldsymbol{E}$ the elastic modulus of the pipe material.

Changes in the temperature ϑ (effect 2b) cause a varied pipe volume expressed by

$$V = V_0 \cdot \left(1 + 3 \cdot \alpha \cdot \left(\vartheta - \vartheta_0\right)\right) \qquad \text{(A 2.3)}$$

while $\boldsymbol{\alpha}$ is the linear coefficient of thermal expansion of the pipe material.

Arranging the above three expressions **Eqs. (A 2.1)** through (**A 2.3)**, the real pipe volume is given as a function of temperature and pressure by:

$$V_{IP} = \frac{\pi}{4} \cdot \left[d_i + \frac{\left(p - p_0\right) \cdot d_i^{\,2}}{2 \cdot w \cdot E} \right]^2 \cdot l \cdot \left[1 + 3 \cdot \alpha \cdot \left(\vartheta - \vartheta_0\right)\right] \qquad \text{(A 2.4)}$$

The possibly entrapped air bubbles (effect 4a) reduce this real volume at reference conditions ϑ_0 and $\boldsymbol{p_0}$ by $\boldsymbol{V_{air}}$. This volume of (compressible) air is changing with respect to pressure $\boldsymbol{p}$ and temperature ϑ (effects 4b and 4c) according to the equation of state of ideal gas:

$$V_{air} = V_{air,0} \cdot \frac{p_0}{p} \cdot \frac{\vartheta + 273.15}{\vartheta_0 + 273.15} \qquad \text{(A 2.5)}$$

Considering this effect, the enclosed actual volume of fluid within the interconnecting pipe is to be calculated by

$$V_{IP} = \frac{\pi}{4} \cdot \left[d_i + \frac{\left(p - p_0\right) \cdot d_i^{\,2}}{2 \cdot w \cdot E} \right]^2 \cdot l \cdot \left[1 + 3 \cdot \alpha \cdot \left(\vartheta - \vartheta_0\right)\right] - V_{air,0} \cdot \frac{p_0}{p} \cdot \frac{\vartheta + 273.15}{\vartheta_0 + 273.15} \qquad \text{(A 2.6)}$$

A great advantage of the closed mathematical expression the entire interconnecting pipe system incorporating all depicted effects by one single mathematic expression is, that for uncertainty calculations the effects of correlations influenced by temperature and pressure are considered exactly.

The process input data of **Eq. (A 2.6)** are measured by process control system, the other data for material properties and dimensions are taken from appropriate tables. Both types of data are affected by measurement uncertainties. Thus an uncertainty calculation has to provide knowledge of the total uncertainty of the calculation of the volume of interconnecting pipe. For a typical set of detailed determined and realistic estimated data:

- V_{IP} = 0.501 m³, V_{air} = 0.001 m³, w = 0.003 m, $E = 1.95 \cdot 10^{11}$ N/m²,
- $\alpha = 15 \cdot 10^{-6}$ m/(mK), ϑ_0 = 20 °C, ϑ = 22 °C, p_0 = 1.0 bar, p = 3 bar;

Table 2 *Interconnecting pipe, interaction of pipe and fluid, sources of uncertainty and their contribution to the expanded uncertainty of interconnecting pipe mass*

Source	Dimension	Quantity	Distribution Divisor	Sensitivity Coefficient	Sensitivity Coefficient	Uncertainty m³
ΔV	m³	0.001	Rectangular 1.73	$c_{VPipe} = \frac{\partial V_{IP}}{\partial V}$	1 m³/m³	5.7812E-4
ΔV_{air}	m³	0.001	Rectangular 1.73	$c_{Vair} = \frac{\partial V_{IP}}{\partial V_{air}}$	-3.3856E-1 m³/m³	1.9570E-4
$\Delta\vartheta$	°C	0.6	Rectangular 1.73	$c_t = \frac{\partial V_{IP}}{\partial t}$	1.9108E-5 m³/°C	6.6272E-6
$\Delta\vartheta_0$	°C	0.6	Rectangular 1.73	$c_{t0} = \frac{\partial V_{IP}}{\partial t_0}$	-1.9085E-5 m³/°C	6.6190E-6
Δp	Pa	5000	Rectangular 1.73	$c_p = \frac{\partial V_{IP}}{\partial p}$	3.5097E-9 m³/Pa	1.0144E-5
Δp_0	Pa	5000	Rectangular 1.73	$c_{p0} = \frac{\partial V_{IP}}{\partial p_0}$	-1.0163E-8 m³/Pa	2.9373E-5
$\Delta\alpha$	1/°C	$1 \cdot 10^{-6}$	Rectangular 1.73	$c_\alpha = \frac{\partial V_{IP}}{\partial \alpha}$	3.0066E+0 m³/(1/°C)	1.7379E-6
ΔE	N/m²	$0.1 \cdot 10^{11}$	Rectangular 1.73	$c_E = \frac{\partial V_{IP}}{\partial E}$	1.4277E-16 m³/(N/m²)	8.2426E-7
Δw	m	0.0005	Rectangular 1.73	$c_w = \frac{\partial V_{IP}}{\partial w}$	-9.2688E-3 m³/m	2.6788E-6
Combined uncertainty			k = 1			**6.1121E-4**
Expanded combined uncertainty			k = 2			**1.2224E-3**

the combined uncertainty was computed as follows. The results of this calculation are depicted in **Table 2** and **Fig. A.3**. The input data are known within upper and lower limits and a rectangular distribution is applied for the computation as shown in **Table 2**.

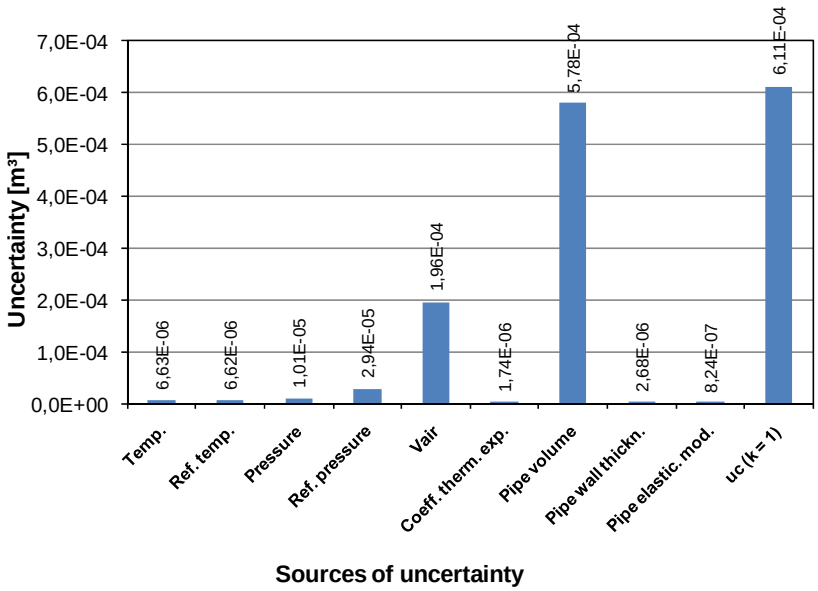

Figure A.3 *Uncertainties in the volume: interaction of pipe and fluid effects*

The change of the interconnecting pipe volume is given by the difference due to varying operating conditions at start and finish in temperature and pressure during the time of the measurement run and has exactly to be computed as the difference between **start** and **finish process conditions** by the following expression:

$$\Delta V_{IP} = V(\vartheta_{finish}, p_{finish}) - V(\vartheta_{start}, p_{start}) \qquad \text{(A 2.7)}$$

Applying **Eq. (A2.6)**, this expression is, in detail, completed as follows:

$$\Delta V_{IP} = \left[\frac{\pi}{4}\cdot\left[d_i + \frac{(p_{finish} - p_0)\cdot d_i^{\,2}}{2\cdot w\cdot E}\right]^2 \cdot l\cdot\left[1+3\cdot\alpha\cdot(\vartheta_{finish} - \vartheta_0)\right] - V_{air,0}\cdot\frac{p_0}{p_{finish}}\cdot\frac{\vartheta_{finish}+273.15}{\vartheta_0+273.15}\right] - \ldots.$$

$$\ldots. - \left[\frac{\pi}{4}\cdot\left[d_i + \frac{(p_{start} - p_0)\cdot d_i^{\,2}}{2\cdot w\cdot E}\right]^2 \cdot l\cdot\left[1+3\cdot\alpha\cdot(\vartheta_{start} - \vartheta_0)\right] - V_{air,0}\cdot\frac{p_0}{p_{start}}\cdot\frac{\vartheta_{start}+273.15}{\vartheta_0+273.15}\right] \qquad \text{(A 2.8)}$$

When applying the well known calculation procedure for the uncertainty computation of the IP volume difference, the result yields in a nearly error-free determination of the volume difference of 1.7E-5 m³ as shown in **Fig. A.4**. This result is obviously wrong because of the numeric subtraction corresponding terms are compensating each other. This pretends an unrealistic accuracy.

In such cases a **Monte-Carlo** based calculation for determining the combined uncertainty is a better choice. This was applied to **Eq. (A 2.1.8)** using the same input data. As the result a realistic value for the combined uncertainty (k =1) of $8.1\cdot10^{-4}$ m³ is achieved in good agreement to the above value of $6.1\cdot10^{-4}$ m³ for the single volume determination. Thus - to keep a closed mathematic expression of the entire system - for further calculations the uncertainty contributions for pipe volume uncertainty determination only are considered as follows:

$$\Delta V_{IP} = \frac{\pi}{4} \cdot \left[d_i + \frac{(p - p_0) \cdot d_i^{\,2}}{2 \cdot w \cdot E} \right]^2 \cdot l \cdot \left[1 + 3 \cdot \alpha \cdot (\vartheta - \vartheta_0) \right] - V_{air,0} \cdot \frac{p_0}{p} \cdot \frac{\vartheta + 273.15}{\vartheta_0 + 273.15} - V_{start} \quad \text{(A 2.1.9)}$$

while $V_{start} = const. = V(\vartheta_{start}, p_{start})$ at start conditions.

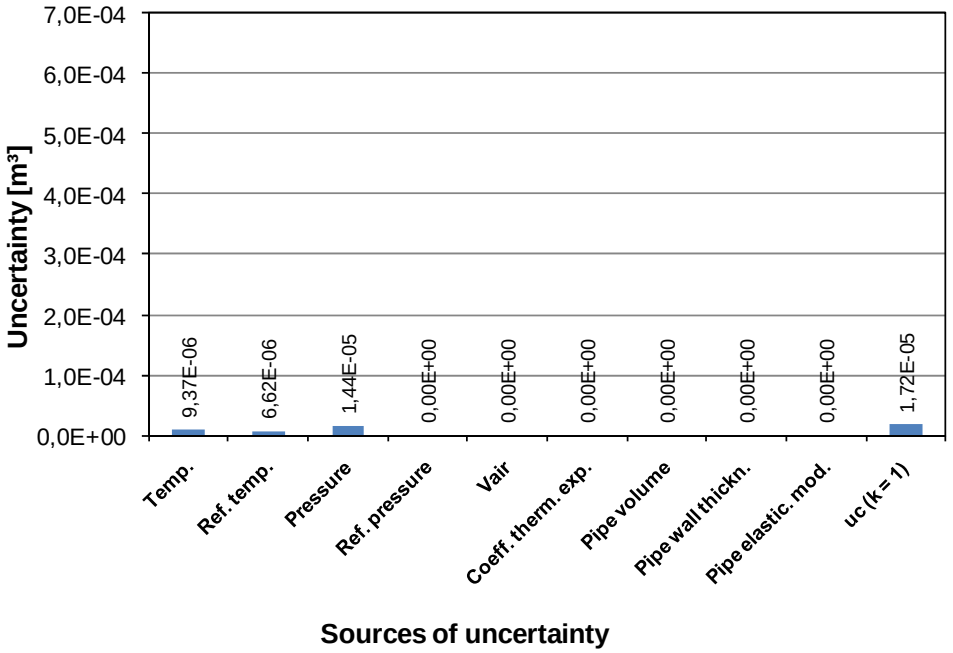

Figure A.4 *Uncertainties of the volume difference: interaction of pipe and fluid effects*

Appendix A.3. Sources of water samples that were incorporated in experimental water density analysis and for deriving approximation functions

In order to determine a practical approximation function for the density-temperature relation that is reasonably applicable in liquid flow calibrations utilizing water as test fluid, a greater number of water samples were analyzed under this aspect. Such a practical approximation function should reveal, as demonstrated in **Appendix A1**, the lowest polynomial degree that is applicable in practical water density measurement and uncertainty analysis.
The series of water samples that were incorporated in the analysis comprised natural origins, eg. glacier water, but in the majority there were "artificial" origins like water in test facilities or others that were taken from water supply systems in several cities and communities in Germany (See: **Table A3**).

Table A3 *.Sources of the water samples that were subject of analysis and density modeling*

No. of sample	Sources of the water samples
1	City of **Dresden**, local water supplier
2	**ISO** / TR 3663 [9]
3	**TANAKA** [4]
4	**TANAKA**, consideration of diss. air[4]
5	**TANAKA**, consideration of comp. 3 bar [4]
6	**ISO 4185** [8]
7	City of **Dresden**, local water supplier
8	Facility of accred. lab, **DKD-K-4090**
9	Facility of accred. lab, **DKD-K-39501**
10	Town of **Lemgo**, local water supplier
11	Facility of flowmeter **manufacturer #1**
12	Facility of accred. lab, **DKD-K- 33901**
13	Facility of accred. lab, **DKD-K- 03901**
14	Town of **Oldenburg**, local water supplier (D)
15	Facility of accred. lab, **DKD-K- 18101**
16	Facility of accred. lab, **DKD-K- 18101**
17	Facility of accred. lab, **DKD-K-46001**
18	Facility of flowmeter **manufacturer #1**
19 … 27	**PTB** Braunschweig
28	Community of **Ottenstein**, local water supplier, Lower Saxony (D)
29	City of **Basel**, local water supplier
30	Community of **Brockhöfe**, local water supplier, Lower Saxony (D)
31	Community of **Ottenstein**, local water supplier, Lower Saxony (D)
32	**St. Christopher glacier**, Austrian Alps
33	Facility of accred. lab, **DKD-K-36701**
34	Facility of flowmeter **manufacturer #1**